American Journal of Applied Sciences

Original Research Paper

Mass Production of Uniformly Sized Air-Filled Poly-Lactic Acid Microcapsules Made from Microbubble Templates

[1]Jay Molino, [1]Svetlana Jojlova, [2]Hirofumi Daiguji and [3]Fumio Takemura

[1]Department of Biomedical Engineering, Universidad Especializada de las Américas, Paseo Albrook, 00629 Panamá, Panamá
[2]Department of Mechanical Engineering, The Univerity of Tokyo, 7-3-1, Hongo, Bunkyo-Ku, Tokyo 113-8656, Japan
[3]National Institute of Industrial Sciences and Technology, Umezono 1-1-1, Tsukuba, Ibaraki, 305-8568, Japan

Article history
Received: 01-02-2019
Revised: 29-07-2019
Accepted: 16-08-2019

Corresponding Author:
Jay Molino
Department of Biomedical Engineering, Universidad Especializada de las Américas, Paseo Albrook, 00629 Panamá, Panamá
Email: jay.molino@udelas.ac.pa

Abstract: Hollow poly(Lactic Acid) (PLA) microcapsules were fabricated using the bubble template method. In this method, microbubbles nucleated inside droplets of a dichloromethane solution of PLA which were located in a continuous phase of poly(vinyl alcohol). PLA-covered microbubbles formed when PLA adsorbed to the bubble surface by physisorption. Then, the coated microbubbles were spontaneously released from the droplet´s interior into the continuous phase. To increase the production yield of hollow microcapsules in this method, ultrasound was applied to enhance bubble nucleation inside the droplets. Thus to attain uniform hollow PLA microcapsules, the optimum PLA concentration with ultrasound was 30 g L^{-1}, which is higher than that without ultrasound (2 g L^{-1}). At the optimum concentration, the average radius was 0.54 μm, with a polydispersity index of 21.2%. It was found that the equilibrium size of the microbubble template radius was the same with and without ultrasound. The production yield had a tenfold increase when ultrasound was employed.

Keywords: Biodegradable Microcapsules, Drug Delivery, Mass Production of Hollow Capsules, Microencapsulation, Ultrasound Enhanced Fabrication, Ultrasound Contrast Agents

Introduction

Ultrasound has proven to be a reliable, low-cost, fast and simple method in bioimaging, medical diagnoses and treatment (Schutt *et al*., 2003; Unger *et al*., 2004; Raisinghani and DeMaria, 2002; Nanda *et al*., 2003). Such a technique has the advantage that it can be applied without damaging the human tissue and can be focused to specific depths between tissues. The clarity of the image can be enhanced via Ultrasound Contrast Agents (UCAs). In this regard, microbubbles are the most effective type of ultrasound contrast agent for biomedical imaging (Stride and Saffari, 2003; De Jong and Hoff, 1993; Lin *et al*., 2009) due to their high acoustic impedance. The applied medical frequency is in the order of 10^6 Hz, which allows the bubble to vibrate at the fundamental frequency. Furthermore, visualization can also be attained from the reading of the harmonic frequencies which in fact are preferred since these differ greatly from those of human tissue. Therefore, having uniformly sized microbubbles is desirable to obtain a narrower backscatter signal. Still, bubbles can also be employed for a number of ablation techniques which are currently in use to treat cancer (e.g., RF ablation and high intensity focused ultrasound, HIFU) (Miller and Song, 2003).

The challenge is that microbubbles (or free bubbles) dissolve quickly in the blood after intravenous infusion (Schutt *et al*., 2003; Sboros, 2008; Leighton, 1994; Ferrara *et al*., 2006), which can be addressed by using a heavy gas to reduce the probability of gas diffusion into the surrounding, continuous (liquid) phase and thus, increase the microbubble lifetime (De Jong and Hoff, 1993). Yet, if they are intended to be employed for prolonged periods (min), the inclusion of a shell (i.e., 10-200 nm thick) composed of lipids or polymers is required to enhance its useful life (Sboros, 2008). The engineering trade-off for extending its lifetime via a shell is a reduction in the energy reflected by the microbubbles at the resonant frequency and its corresponding harmonics. In other words, the backscatter of sound is greater at the gas-liquid interface (bubble-liquid interface) compared to a liquid-liquid interface if the bubble is wrapped by a surfactant or by stabilizing flexible material (De Jong and Hoff, 1993; Gorce *et al*., 2000; Hoff *et al*., 2002; Shankar *et al*., 2002).

Science Publications

© 2019 Jay Molino, Svetlana Jojlova, Hirofumi Daiguji and Fumio Takemura. This open access article is distributed under a Creative Commons Attribution (CC-BY) 3.0 license.

The second constraint is that microbubbles should lie within 1-4 μm size range to effectively pass through the capillary circuit, this guarantees a long-circulating time before it drains into the liver (Lin *et al*., 2009). This last difficulty can be solved by forming thermodynamically stable microbubbles (closed system) (Daiguji *et al*., 2009).

The idea of a microcapsule is not new as it is already present in nature, e.g. vesicular structures and micelles. In the body, the lipid bilayer is stable because water's affinity for hydrogen bonding never stops. It is the hydrogen bonding of water that holds a membrane together (Daiguji *et al*., 2009). However, lipid bilayers have limitations since if they are to be employed to stabilize microbubble they will easily disintegrate as the interaction between the lipids molecules is weak, furthermore, these layers are not so useful for engineering applications. But with the development of new techniques, biologically compatible microcapsules, as well as capsules suited for several kinds of engineering application, can be created (Molino Cornejo, 2019).

Even though there are several techniques to synthesize hollow microcapsules, in general, all of them can be classified into four main synthesis methods namely: chemical methods, physicochemical methods, electrochemical and physicomechanical methods. Among the chemical methods, the interfacial polymerization method is the most popular. In this technique, the capsule shell is the result of a reaction among the polymer chain and the surface of a droplet or a solid particle that it's being used as a core. In most cases, multifunctional monomers, i.e. isocyanates, are dispersed in the liquid cores, which are suspended in a dispersing/emulsifying continuous phase. Another reactant multifunctional polymer (e.g., amine) is dispersed in the continuous phase and this allows the reaction of both multifunctional polymers to take place at the droplet-dispersing phase (rapid polymerization at the interface), then the cores are removed to attain a hollow capsule. Polymerization can also occur at a bubble surface and therefore hollow microcapsules are immediately created with a polymer shell (Saihi *et al*., 2006; Feng *et al*., 2007). Nonetheless, we devised a method in which a thin layer of PLA was directly adsorbed, thus, rendering a hollow biodegradable microcapsule from a bubble template without the need of surfactants (Molino Cornejo, 2019). This original process doesn't require any external forces to produce hollow microcapsules as it relies on solvent evaporation (Daiguji *et al*., 2009). These microcapsules can also be employed for therapeutic purposes in areas of drug delivery, gene therapy, or as cell carriers for tissue engineering (Shi *et al*., 2009; Malda and Frondoza, 2006; Zhang *et al*., 2009; Klibanov, 2006). We named this technique the bubble template method. The challenge we face with this fabrication process is, even though it yields uniformly sized microcapsules, that it is not optimized for mass production.

In this study, we employed ultrasound in the kHz range to enhance microbubble nucleation in the droplet's interior. Based on the number density of nucleated bubbles and released bubbles from the droplet's interior, the kinetics of the bubble release is discussed. Furthermore, the effect of the application of ultrasound on the size of nucleated microbubbles and the size of the final capsules with respect to the initial concentration of PLA, c_{PLA}, is disclosed. It is important to highlight that ultrasound is a technique mainly used to trigger drug release from the capsule, not to fabricate them (Klibanov, 2006; Zhu *et al*., 2010). This paper focuses on the mass production of microcapsules made from microbubble templates using ultrasound.

Materials and Methods

Materials

The following chemicals were used: A 2kDa PLA (i.v. 0.1-0,2) from Polyscience, U.S.; methylene chloride (CH_2Cl_2) with a 99.99% purity from Wako Pure Chemical Industries, Ltd., Japan; PVA-Gohsenal T-350 from Nippon Gohsei, Japan, water from a Milli-Q Advantage A10 water purification system.

Methods

The following two fabrication processes were employed:

Method A (Standard Process)

In a petri dish containing a 2% (w/w) PVA_{aq} solution, ten 20 μL droplets of a CH_2Cl_2 solution of PLA at various initial concentrations were placed via microsyringe (Daiguji *et al*., 2009). Immediately, methylene chloride started to diffuse into the continuous phase which allowed microbubbles to nucleate inside the droplet. As it was found in our previous (Daiguji *et al*., 2009; Molino Cornejo *et al*., 2011), since the solubility of air in the aqueous solution is smaller than in the oil phase, the air did not diffuse to the outside of the droplet but instead nucleated in the inside forming thermodynamically stable microbubbles. Afterward, PLA adsorbed to the microbubble surface which resulted in PLA covered microbubbles being released from the droplet interior into the PVAaq solution. The solidified microcapsules were collected, purified and dried using water from a *Millipore System* (18.2 MΩ.cm at 25C TOC < 5 ppb) and to remove any contaminant from the PLA shell. If the purification process was not thorough, PVA was not properly removed from the shell. To completely dry the capsules, a desiccator at 0.7 kPa with silica gel beads was employed. The drying process lasted 36 h. Finally, the refined product, hollow microcapsules, was obtained in the form of fine white powder.

Method B (Process Under Sonication)

The process is similar to the one described in *Method A*. However, after forming the droplets in the petri dish, the dish was placed in the middle of an ultrasonic bath (*AS ONE ultrasonic bath*) which contained water which dimensions are 230×20×152 mm (L×W×D). The output frequency and power (a low power unit) of the ultrasonic bath was 38 kHz and 35 W, respectively. The water level was approx. 120 cm. The pressure due to the acoustic wave was measured with a Jowa PT300 immersible pressure transducer at five different positions inside the ultrasonic bath using the transducer: The four corners and at the middle at a depth from the water surface of 5mm. We were more interested at the surface level since the petri dish with the droplets was located at the surface level (approximate depth of 5 mm).

The temperature in the ultrasonic bath peaked at 35°C (the boiling temperature of methylene chloride is 40°C). During the application of ultrasound, the droplet's color turned cloudy, which was a clear indication that microbubble nucleation was taking place. The samples were continuously sonicated until the droplets dissolved completely into the continuous phase. The purification process was the same as the one described in *Method A*.

Interfacial tension measurements were performed via the pendant drop method using the *Drop Master Series DM-501* (Kyowa Interface Science, Japan) to confirm that the surface tension at the liquid-liquid interface (CH_2Cl_2-PVA) was not affecting the release of the microbubbles. For this purpose, CH_2Cl_2 drops with an initial PLA c_{PLA}, of 2 and 30 g L^{-1} were formed in a 2% (w/w) PVA aqueous solution. The volume of the drops was kept constant at 10 µL and the interfacial tension was monitored for at least 30 min. The temperature of the experiments was 298 K. Top and Bottom of Fig. 1 show the time courses of interfacial tension and droplet volume for each of the solutions of PLA, respectively.

The measured interfacial tensions at 30 min were 1.26×10^{-2} and 1.35×10^{-2} N m^{-1}, respectively, for c_{PLA} = 2 and 30 g L^{-1}. The time variation of the surface tension and volume of the droplet is shown in Fig. 4. This reveals that the energy required for capsule release (Molino Cornejo *et al*., 2011) is not affected by the initial c_{PLA}. The experiments were performed at room temperature.

An inverted microscope (*Nikon ECLIPSE Ti-E*) was employed to confirm: a. the effect of ultrasound on the total amount of nucleated microbubbles, b. the effect of ultrasound on the final size of the microcapsules and c. elucidate the mechanism of release of PLA coated microbubbles from the droplet's interior. The experiments were performed at room temperature, 298 K. The polymer was tagged with Nile Red to confirm that the microcapsules were hollow (Daiguji *et al*., 2009).

To observe the fabricated microcapsules, an FE-SEM (*S-4800*, Hitachi High-Technologies, Japan) was used. Prior to the FE-SEM measurements, the microcapsules were freeze-dried for 6 h and then frozen with liquid nitrogen (-196°C).

Finally, for the statistical analysis, we determined the Cronbach's alpha, to measure the internal consistency of both fabrication methods (comparison of the resultant capsules size), the average size and the standard deviation of the capsules fabricated using both methods, Microsoft Excel was employed.

A schematic of the fabrication process is shown in Fig. 2.

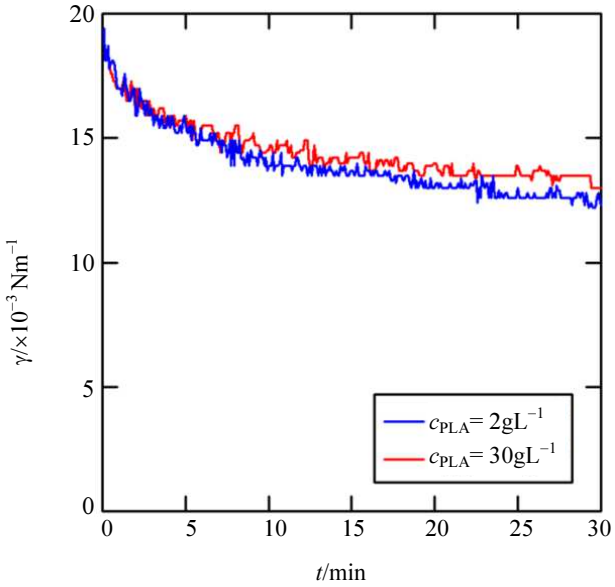

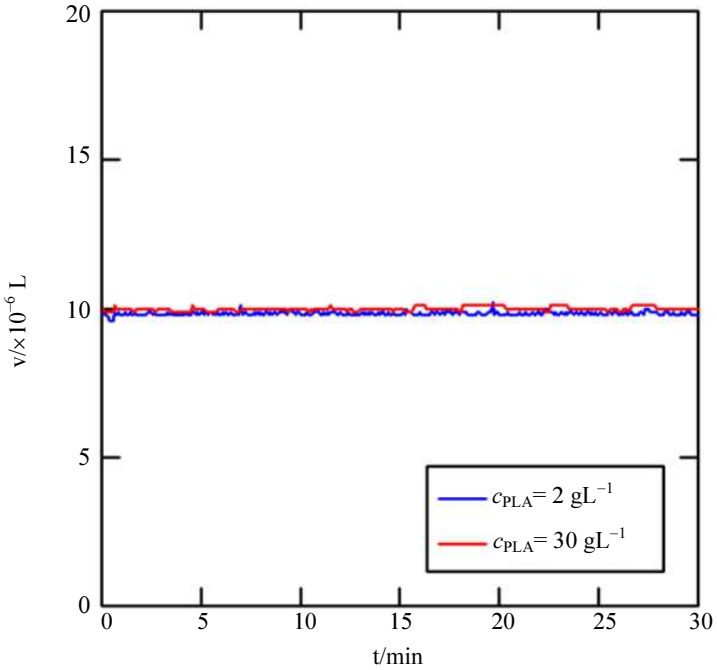

Fig. 1: Time courses of interfacial tension, γ, (top) and droplet volume, *v*, (bottom) of a c_{PLA} of either 2 or 30 g L^{-1}. The droplet was CH_2Cl_2 solutions of PLA (2 kDa) and the surrounding medium was a 2% (w/w) PVA aqueous solution

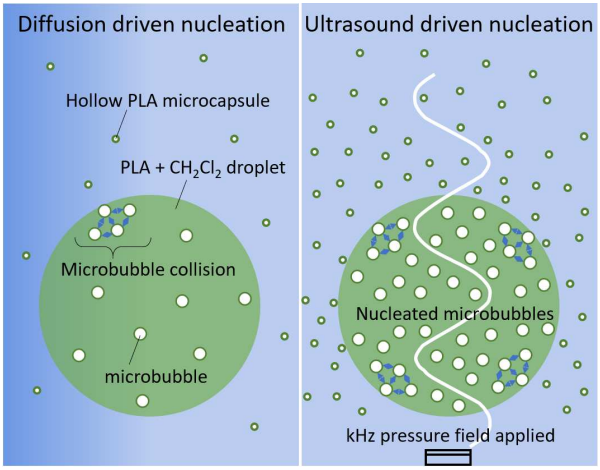

Fig. 2: Left Panel: Diffusion is driven microbubble nucleation. Right Panel: Ultrasound driven nucleation process

Results

Microcapsule Fabrication Via Ultrasound

Figure 3 shows the measured pressure waves on the surface of CH_2Cl_2 droplets in a 2% (w/w) PVA aqueous solution inside a glass dish located at the center of the ultrasonic bath. Water *Location A* and *B* were near the anti-node (center of the ultrasound bath) and node (corners of the ultrasound bath) of the pressure standing wave, respectively. The amplitudes at location A and B were measured to be 70 and 10 kPa, respectively. At both locations, bubble nucleation was enhanced but the droplet remained stable. In this study, hollow PLA capsules were synthesized at *location A* because more microbubbles were observed at this location. However, when the glass dish was located in particular areas at the same water level of either *Location A* or *B*, the droplets were deformed and PLA particles and films were generated at the droplet surface because the applied pressure wave was not a perfect plane wave in the vertical direction. In this study, such placements were avoided.

We successfully fabricated gas-filled PLA microcapsules using ultrasound. Figure 4 shows a typical bright field image of PLA covered microbubbles being released from the methylene chloride droplet´s interior when c_{PLA}=30 g L^{-1}. The observation was performed before (top section of Fig. 4) and right after the ultrasound was applied to the droplets (bottom section of Fig. 4).

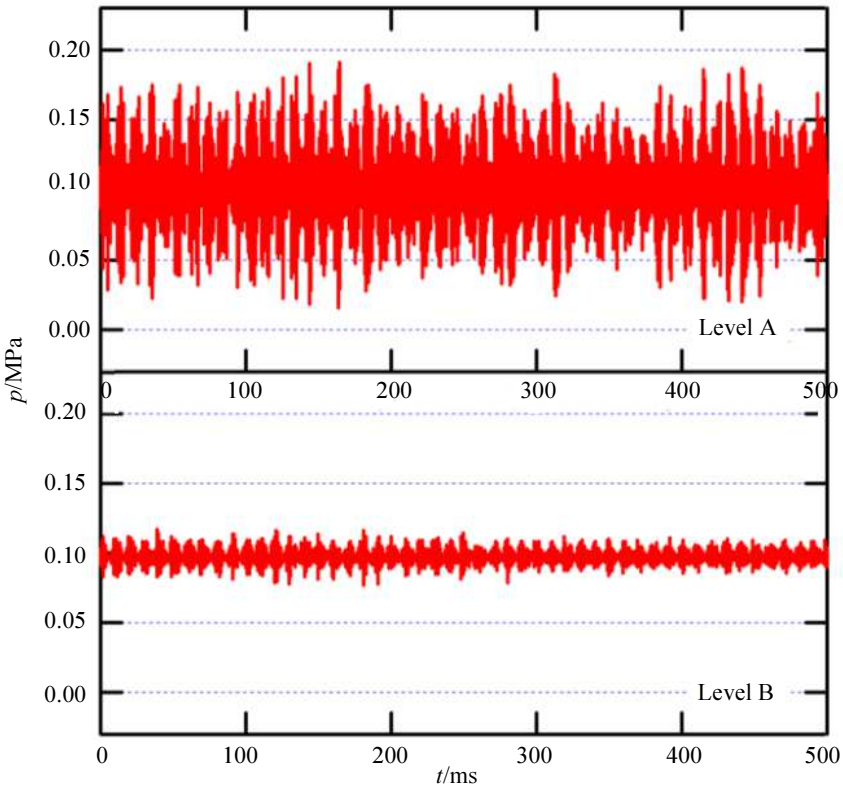

Fig. 3: Pressure waves measured at two different water levels in the ultrasonic bath

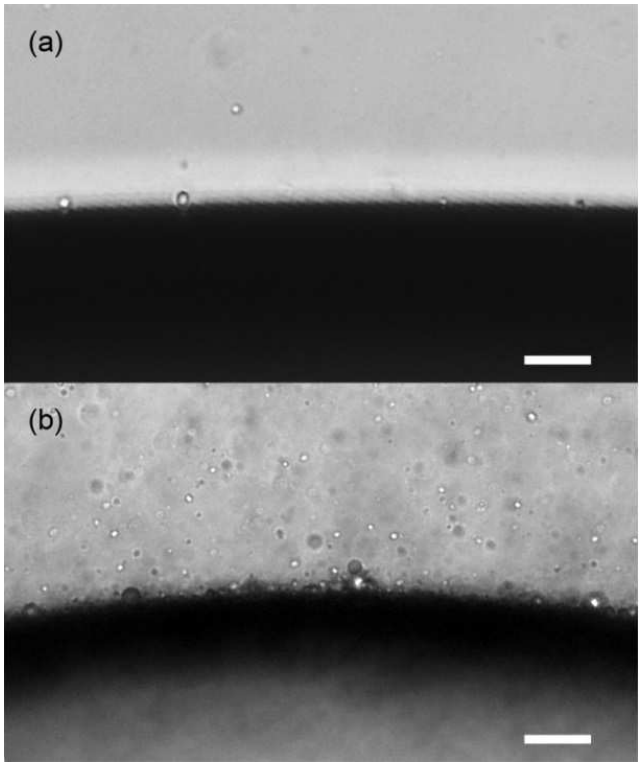

Fig. 4: PLA coated microbubble release from the interior of the droplet: (A). without ultrasound; (B). with ultrasound. c_{PLA} 30 g L^{-1}. The scale bar represents 25µm

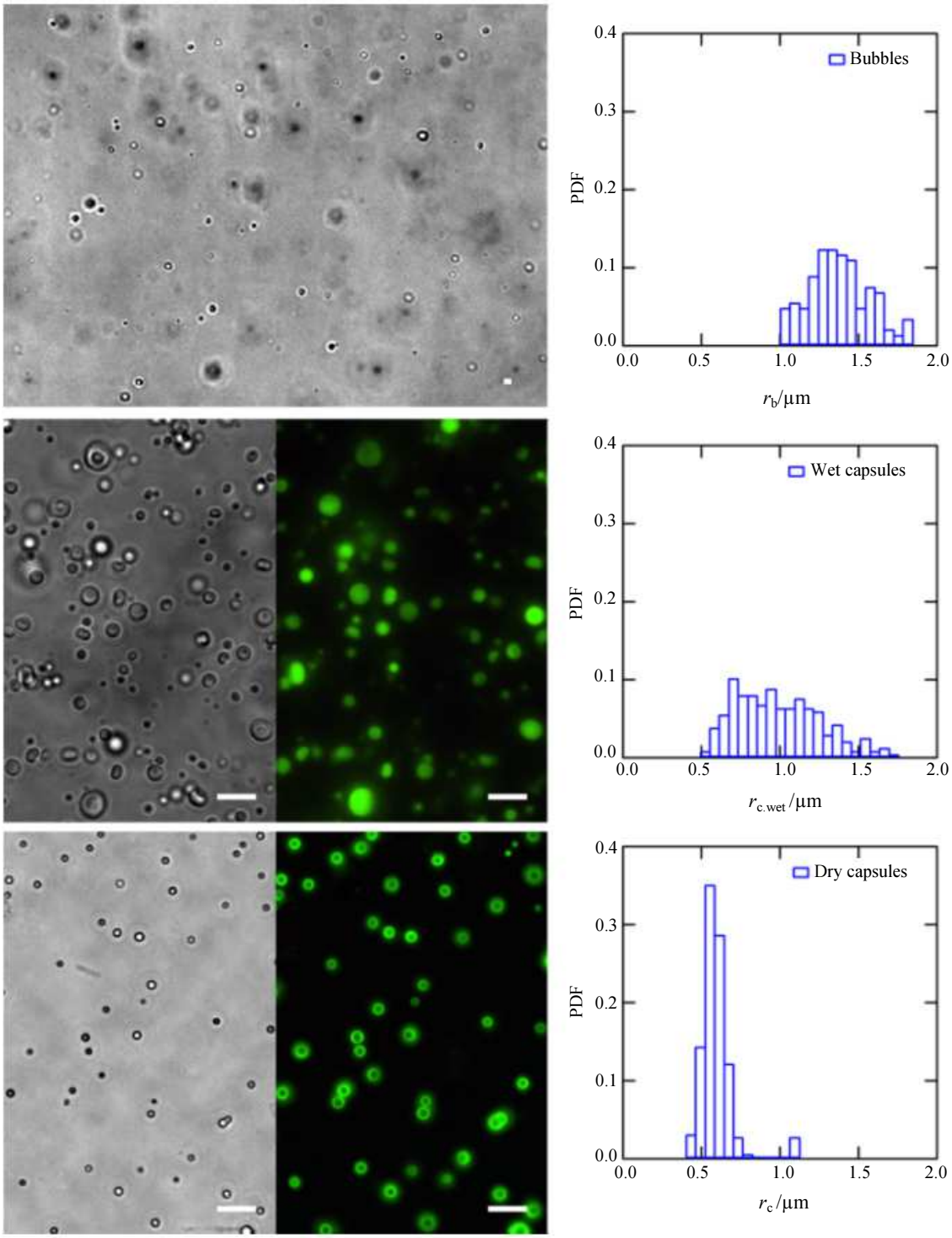

Fig. 5: A bright-field image of microbubbles and the radius distribution inside a droplet of a CH_2Cl_2 solution of PLA when ultrasound was employed (top). Bright-field and fluorescent images of hollow PLA microcapsules and the radius distribution inside 2% (w/w) PVA aqueous solution (middle) and after drying (bottom). The initial concentration of PLA, c_{PLA}, was 30 g L^{-1} and the PLA molecular weight was 2 kDa. The scale bars represent 5 μm

After sonication, the droplets remained cloudy for several minutes. It was found that the number of nucleated microbubbles increased. All measurements were taken at the middle of the droplet where the meniscus effect did not affect the clarity of the image and droplet and, furthermore, to avoid coalesced bubbles that can be located at the top of the droplet due to buoyancy. Such bubbles never become hollow PLA microcapsules mainly due to their size. The average radius for the nucleated microbubbles, its standard deviation and PI (Polidispersivity index = Standard deviation/mean) was 1.34 μm, 0.23 μm and 17.4%, respectively (Daiguji *et al*., 2009).

Figure 5 shows the formation process of microcapsules (top = bubble nucleation, middle = wet capsules, bottom = dry capsules) when c_{PLA}=30 g L^{-1}. The fluorescence (green rings due to the presence of Nile Red), indicates that microcapsule has a hollow interior since the air was not tagged with fluorescein. It is worth to note that the final dried hollow microcapsule had a smaller size compared to the microbubble template. This result was observed in our previous work as well (Molino Cornejo *et al*., 2011).

It is also observed that the vast majority of the capsules created using c_{PLA}=30 g L^{-1} have a single void as it is seen from the figure. The average radius for the microcapsules, its standard deviation and PI of the outer radius were 0.54 μm, 0.11 μm and 21.2%, respectively.

The Effect of Ultrasound

Ultrasound proved to be effective to increase the number of nucleated microbubbles as shown in Fig. 4 as well. The image shows the number of PLA covered microbubbles (microcapsules) being released from the droplet's interior when ultrasound was not applied (*Method A*) and when ultrasound was applied (*Method B*), respectively.

To explain the bubble release mechanism when ultrasound was employed, we first calculated the natural frequency of the microbubbles which is given by the Minnaert formula (Doinikov *et al*., 2009):

$$f_0 = \frac{1}{2\pi r_b}\left(\frac{3\gamma p'}{\rho'} + \frac{2(3\gamma - 1)\sigma}{\rho' r_b}\right)^{1/2} \quad (1)$$

where, f_0 is the natural frequency of a bubble which equilibrium radius is r_b; p' is the hydrostatic pressure in the surrounding liquid; γ is the heat capacity ratio of the gas inside the bubble; σ is the surface tension at the gas-liquid interface; and ρ′ is the equilibrium density of the liquid; and the calculated natural frequency f_0 was 3.4 MHz when the equilibrium radius r_b = 1 μm given that in our study, p'=101.3 kPa, ρ′=1330 kg m^{-3}, σ = 0.0278 N m^{-1} and γ=1.4. Since the frequency of the employed ultrasound was 38 kHz, this wave cannot collapse, nor cavitate a microbubble by itself. Thus the ultrasound only aided the nucleation and furthermore, it cannot produce the calculated large pressure required for releasing the microbubbles from the droplet's interior (Molino Cornejo *et al*., 2011).

Nonetheless, if more bubbles are nucleated and distributed at the liquid-liquid interface, the frequency of bubble release increases due to microbubble collision and thus a specific microbubble would have enough kinetic energy to overcome the energy barrier at the interface. From the micrographs, it was assessed that when ultrasound is applied, the number density of nucleated microbubbles was 10 times larger than in the diffusion-driven process. Likewise, it was measured that the number of fabricated microcapsules was 10 times larger when ultrasound was employed (*Method B).* Ergo, it is plausible to conclude that the number of nucleated microbubbles is directly related to the number of produced microcapsules. The mechanics of release are the same in *Method A* and *Method B*, but the frequency of release differed by a factor of ten.

Equilibrium Bubble Radius

The equilibrium bubble radius, r_b, is given by equation (2):

$$r_b = 2\sigma / p_1'' \quad (2)$$

where, σ is the interfacial tension of a CH_2Cl_2 solution of PLA at the bubble-solution interface and p_1'' is the partial vapor pressure of CH_2Cl_2. It is noted that p_1'' is close to the saturation vapor pressure of pure CH_2Cl_2 at low c_{PLA} and the air pressure inside the bubbles is approximately equal to the liquid pressure. The value of r_b was predicted to be 0.95 μm at low c_{PLA} and 298 K. Except for low c_{PLA} conditions, because the partial vapor pressure varies with its mole fraction in solution, p_1'' should decrease with increasing c_{PLA} (Molino Cornejo *et al*., 2016). However, analysis of the data of microbubbles nucleated with and without ultrasound revealed that there was no statistical difference among the measurements with a Cronbach´s alpha of 0.92; which implies that the size of the bubble is not affected by the presence of the ultrasound when compared to the diffusion only driven process.

Figure 5 shows the outer radius of the fabricated dry hollow PLA microcapsules as a function of c_{PLA} when ultrasound was not applied (*Method A*) or applied (*Method B*).

In *Method A*, the largest and the most uniformly sized capsules could be obtained at c_{PLA}=2 g L^{-1} and the capsule size decreased and the uniformity deteriorated with increasing c_{PLA} (Molino Cornejo *et al*., 2011). When

c_{PLA} was higher than 30 g L^{-1}, most fabricated capsules formed aggregates and thus it was difficult to obtain independent capsules. On the other hand, in *Method B*, the capsule size slightly increased with increasing c_{PLA} but the uniformity did not change so much except for low or high c_{PLA} values. In *Method A*, bubbles nucleated slowly and PLA covered the bubbles completely before the bubble release. Excess PLA could form a highly viscous layer close to the droplet surface, yielding the resistance for the bubble release. Therefore, a c_{PLA} of 2 g L^{-1} was optimum when ultrasound is not applied (solely diffusion-driven nucleation) (Shankar and Krishna, 2002). This is shown in Fig. 6.

On the other hand, in *Method B*, a c_{PLA} of 30 g L^{-1} proved to be optimal. When ultrasound was employed, bubble nucleation was enhanced and thus the total amount of PLA required for completely coating the nucleated bubbles increased. Even at high c_{PLA}, PLA could cover the bubbles rather than form a highly viscous layer at the droplet surface. Therefore, PLA-coated microbubbles could still be released from the droplet's interior under sonication. However, after drying, the average size was smaller, the capsules displayed a smaller size than those fabricated without sonication (*Method A*).

Thus, using ultrasound enabled us to mass produce the microcapsules faster and still with high uniformity. The driving mechanism for bubble nucleation in *Method A* was the diffusion of dichloromethane into the aqueous phase. *Method A* lasted several hours (more than 7h), meanwhile, with *Method B* (ultrasound), it took around 45 min. Figure 7 shows an FE-SEM image of the fabricated capsules via ultrasound for c_{PLA} = 30 g L^{-1}.

It is important to notice that when c_{PLA} is high, the capsule size decreases in the case of diffusion-driven nucleation compared to an ultrasound drove nucleation. This can be well understood from the fact that in a solution, several bubbles below the stable radius form. The higher the concentration of the polymer the easier it is to cover them before they dissolve back into the solution. But when the concentration is high and the nucleation rate increases due to ultrasound, the probability of a microbubbles serving as a nucleation site increases, thus the bubble increases its size and is successfully stabilized since there is plenty of PLA; yet, also very small microbubbles can be rapidly stabilized before it can dissolve back into the solution.

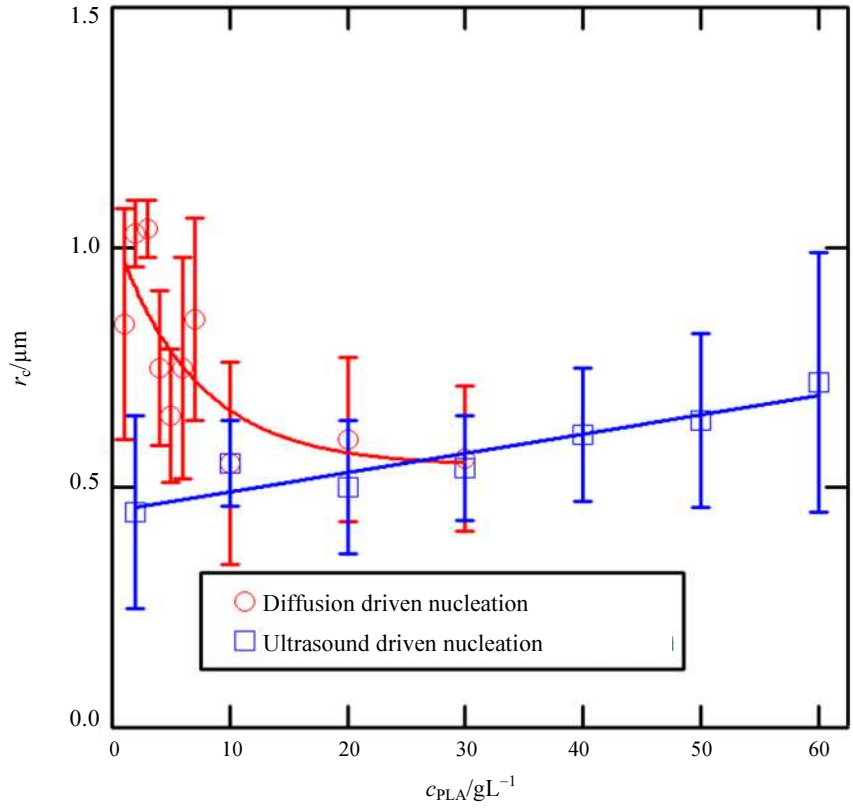

Fig. 6: Microcapsule radius as a function of the initial PLA concentration when ultrasound was not applied (*Method A*) or applied (*Method B*). The molecular weight of PLA was 2 kDa and the aqueous medium was 2% (w/w) PVA aqueous solution

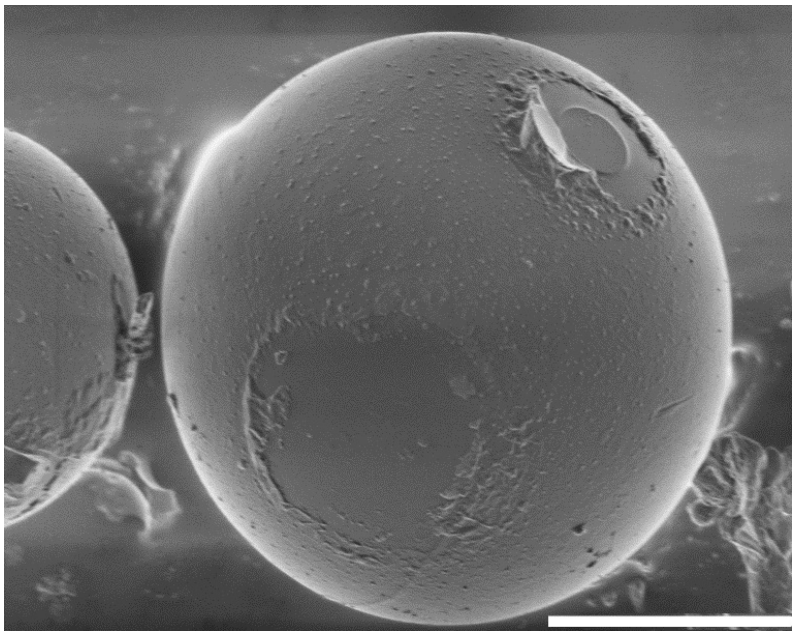

Fig. 7: FE-SEM images of hollow PLA microcapsules fabricated using *Method B* from 2 kDa PLA solutions with c_{PLA} = 30 g L^{-1}. The scale bars represent 0.5 μm

Discussion

Shrunken and Bridged Microcapsules Opatimum c_{PLA}

Upon further observation, the experimental results suggested that the shrinking process occurs as follows: **a.** first, the bubble crosses the liquid-liquid interface and then **b.** the microcapsule dries, which implies that CH_2Cl_2 is removed from the polymer structure allowing it to harden completely. During the first step, inside the droplet of methylene chloride, the polymer prefers a swollen configuration. However, at the first contact with the aqueous continuous phase, the hydrophobic sections of the polymer (PLA) reduce their size in order to minimize the surface area in contact with the continuous phase, thus avoiding any inclusion of H_2O. In addition, since the enclosed gas is a mixture of CH_2Cl_2 and air (the volume ratio of air to CH_2Cl_2 is 0.13 (Molino Cornejo *et al*., 2016), more CH_2Cl_2 gas diffuses into the adjacent continuous aqueous phase. The fact that the capsule shrinks is also credited with the diffusion of CH_2Cl_2 gas into the aqueous phase. When ultrasound was used, bubble nucleation was enhanced and to produce microcapsules, c_{PLA} has to be increased to 30 g L^{-1}. In spite of the increased c_{PLA}, is possible that due to the rate of capsule production, the amount of PLA per bubble could also affect the capsule size. This is if the bubble could not be covered completely with polymer, gas leakage could take place. In addition, the temperature of the gas can increase since mechanical energy (ultrasound) is converted to heat thus affecting the specific volume of the gas inside the bubble templates. When it cools down, the size of the bubble decreases.

As for the second step, the capsule shell is not completely solid. Actually, it is in a gel state due to the presence of CH_2Cl_2. Only in a dry/low-pressure environment or increasing the capsules surrounding temperature will remove CH_2Cl_2 from the polymer structure. Finally, the fabricated hollow PLA microcapsule ends up being smaller than the original bubble template. Indeed the dried capsules are even smaller than the wet ones (Fig. 5).

It was also understood that the rate of appearance of bridged microcapsules increased as c_{PLA} increased in *Method A and Method B*. This is due to the fact that, in a higher viscosity solution, the transferred energy is significantly damped by the viscous medium, which allows PLA-covered microbubbles to remain for a longer period at the liquid-liquid interface. Indeed, because solvent diffusion takes place, a viscous layer appears at the interface inside the droplet (which also increases its thickness with time). This layer displays different rheological properties compared to the bulk solution (Rubinstein and Colby, 2003; Alerts *et al*., 2007; Duenweg, 2018). De Gennes (2002) provided a theoretical discussion regarding this layer, which is considered an elastic layer in the sol-gel transition. Accordingly, the outmost part of this layer (the one close to the liquid-liquid interface) can and will solidify into a solid film. Therefore, the initial c_{PLA} is an important indicator, as it determines the time required to achieve such viscous conditions which, agglomerates PLA-covered microbubbles at the interface.

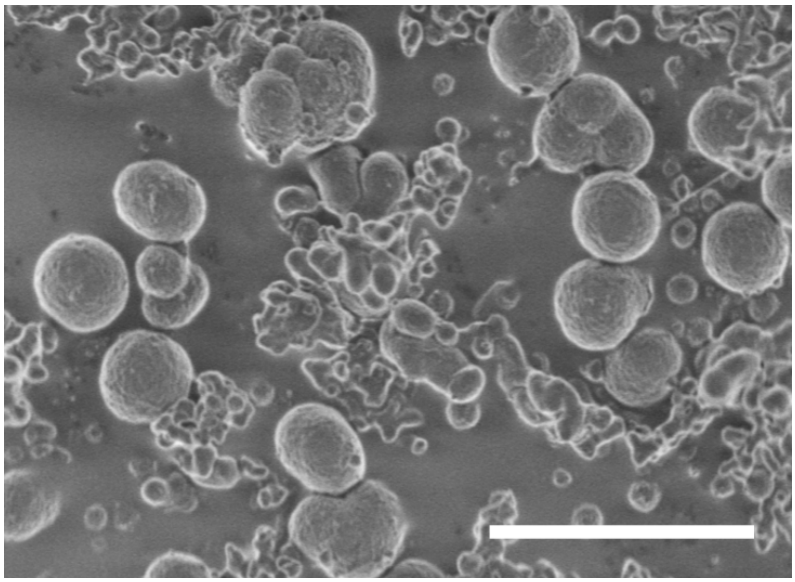

Fig. 8: FE-SEM images of hollow PLA microcapsules fabricated using process A from 2 kDa PLA solutions with c_{PLA} = 70 g L^{-1}. The scale bars represent 25 μm

When sufficiently strong energy can be transferred to the agglomerated capsules, they are released, solidify and become bridged capsules, as confirmed in Fig. 8. It is worth to mention that particles are also manufactured when a high c_{PLA} is used.

Conclusion

It was shown that ultrasound can be effectively employed to mass-produce hollow PLA microcapsules without compromising uniformity. The frequency of bubble release for the ultrasound driven nucleation was higher compared to the diffusion driven process. The optimum concentration of PLA with sonication was 30 g L^{-1}, which was higher than the optimum concentration of 2g L^{-1} in the standard bubble template method without sonication. It was also proven that the final microcapsules given the optimum PLA concentration for each fabrication method, were statistically the same.

Future work focuses on: (1.) The in vitro analysis of the acoustic properties of the microcapsules, the degradation kinetics and the mechanical characterization (e.g. nanoindentation) of the capsules must be performed in detail. (2.) Future studies should also analyze mass transport through the polymer shell in several flow conditions that characterize blood flow in human bodies (vessels, capillaries, blood clots, etc). It is possible to load the capsules with hydrophobic drugs, however, our fabrication method can be adjusted to load hydrophilic drugs. (3.) Furthermore, our process can be potentially employed for manufacturing inorganic capsules that can serve as acoustic or heat insulator systems.

Acknowledgment

A special thanks to the technicians and colleagues at Daiguji Thermal Engineering Laboratory for their support.

Funding Information

This research was supported by both, the Universidad Especializada de Las Américas (UDELAS, Republic of Panama), research grant No. 009-2017 and by the Japanese Society for the Promotion of Science (JSPS), research grant No.201306917.

Authors Contributions

Professor Svetlana focused on the statistical analysis of the data. As for the other authors, they collaborated equally (experiment design and writing) in the completion of the present study.

Ethics

This article is original and contains unpublished material. The corresponding author confirms that all of the other authors have read and approved the manuscript and no ethical issues involved.

References

Alerts, M., A. Tracking, B. Tracking, B. Sciences, B. Sciences and C. Science *et al*., 2007. Neutron spin echo spectroscopy viscoelasticity rheology. Neutron Spin Echo. Spectrosc Viscoelasticity Rheol.

Daiguji, H., S. Takada, J.J.M. Cornejo and F. Takemura, 2009. Fabrication of hollow poly(lactic acid) microcapsules from microbubble templates. J. Phys. Chem. B. DOI: 10.1021/jp9053956

De Gennes, P.G., 2002. Solvent evaporation of spin-cast films: Crust effects. Eur. Phys. J. E., 7: 31-4. DOI: 10.1140/epje/i200101169

De Jong, N. and L. Hoff, 1993. Ultrasound scattering properties of Albunex microspheres. Ultrasonics. 31: 175-81. DOI: 10.1016/0041-624X(93)90004-J

Doinikov, A.A., J.F. Haac and P.A. Dayton, 2009. Resonance frequencies of lipid-shelled microbubbles in the regime of nonlinear oscillations. Ultrasonics [Internet], 49: 263-8. DOI: 10.1016/j.ultras.2008.09.006

Duenweg, B., 2018. Polymer solutions [Internet].

Feng, Z., Z. Wang, C. Gao and J. Shen, 2007. Hollow microcapsules with a complex polyelectrolyte shell structure fabricated by polymerization of 4-vinyl pyridine in the presence of poly(sodium 4-styrene sulfonate) and silica particles. Mater Lett., 61: 2560-4. DOI: 10.1016/j.matlet.2006.09.057

Ferrara, K., R. Pollard and M. Borden, 2006. Ultrasound microbubble contrast agents: Fundamentals and Application to Gene and Drug Delivery. Annu. Rev. Biomed. Eng., 9: 415-47. DOI: 10.1146/annurev.bioeng.8.061505.095852

Gorce, J.M., M. Arditi and M. Schneider, 2000. Influence of bubble size distribution on the echogenicity of ultrasound contrast agents: A study of sonovue(TM). Invest Radiol., 35: 661-71. DOI: 10.1097/00004424-200011000-00003

Hoff, L., P.C. Sontum and J.M. Hovem, 2002. Oscillations of polymeric microbubbles: Effect of the encapsulating shell. J. Acoust Soc. Am., 107: 2272-80. DOI: 10.1121/1.428557

Klibanov, A.L., 2006. Microbubble contrast agents: Targeted ultrasound imaging and ultrasound-assisted drug-delivery applications. Invest Radiol., 41: 354-62. DOI: 10.1097/01.rli.0000199292.88189.0f

Leighton, T., 1994. The acoustic bubble [Internet]. Academic Press. Academic Press.

Lin, P.L., R.J. Eckersley and E.A.H. Hall, 2009. Ultra bubble: A laminated ultrasound contrast agent with a narrow size range. Adv. Mater., 21: 3949-52. DOI: 10.1002/adma.200901096

Malda, J. and C.G. Frondoza, 2006. Microcarriers in the engineering of cartilage and bone. Trends Biotechnol., 24: 299-304. DOI: 10.1016/j.tibtech.2006.04.009

Miller, D.L., J. Song, 2003. Tumor growth reduction and DNA transfer by cavitation-enhanced high-intensity focused ultrasound *in vivo*. Ultrasound Med. Biol., 29: 887-93. DOI: 10.1016/S0301-5629(03)00031-0

Molino Cornejo, J.J., D. Sakurai, H. Daiguji and F. Takemura, 2016. Effect of dissolved poly(lactic acid) on the solubility of CO2, N2 and He Gases in dichloromethane. J. Chem. Eng. Data., 61: 94-101. DOI: 10.1021/acs.jced.5b00268

Molino Cornejo, J.J., H. Daiguji and F. Takemura, 2011. Factors affecting the size and uniformity of hollow poly(lactic acid) microcapsules fabricated from microbubble templates. J. Phys. Chem. B., 115: 13828-34. DOI: 10.1021/jp208056b

Molino, J., 2019. Microcápsulas vacías empleadas en aplicaciones de ultrasonidos: Generalidades, Usos y Métodos de Fabricación. Eur. Sci. J. ESJ., 15: 394-424. DOI: 10.19044/esj.2019.v15n12p394

Nanda, N.C., D.W. Kitzman, H.C. Dittrich and G. Hall, 2003. Delineation, inter-reader agreement and the accuracy of segmental wall motion assessment. Echocardiography, 20: 121-128. DOI: 10.1046/j.1540-8175.2003.03014.x

Raisinghani, A. and A.N. DeMaria, 2002. Physical principles of microbubble ultrasound contrast agents. Am. J. Cardiol., 90: 3-7. DOI: 10.1016/S0002-9149(02)02858-8

Rubinstein, M. and R.H. Colby, 2003. Polymer Physics. 1st Edn., OUP Oxford, New York, ISBN-10: 019852059X, pp: 456.

Saihi, D., I. Vroman, S. Giraud and S. Bourbigot, 2006. Microencapsulation of ammonium phosphate with a polyurethane shell. Part II. Interfacial polymerization technique. React. Funct. Polym., 66: 1118-25. DOI: 10.1016/j.reactfunctpolym.2006.02.001

Sboros, V., 2008. Response of contrast agents to ultrasound. Adv. Drug Deliv. Rev., 60: 1117-36. DOI: 10.1016/j.addr.2008.03.011

Schutt, E.G., D.H. Klein, R.M. Mattrey and J.G. Riess, 2003. Injectable microbubbles as contrast agents for diagnostic ultrasound imaging: The key role of perfluorochemicals. Angew Chemie-Int Ed., 42: 3218-35. DOI: 10.1002/anie.200200550

Shankar, PM., P.D. Krishna and V.L. Newhouse, 2002. Subharmonic backscattering from ultrasound contrast agents. J. Acoust Soc. Am., 106: 2104-10. DOI: 10.1121/1.428142

Shi, X., L. Sun, J. Jiang, X. Zhang and W. Ding, Z. Gan, 2009. Biodegradable polymeric microcarriers with a controllable porous structure for tissue engineering. Macromo. Biosci., 9: 1211-8. DOI: 10.1002/mabi.200900224 8.

Stride, E., N. Saffari, 2003. Microbubble ultrasound contrast agents: A review. Proc. Inst. Mech. Eng. Part H J. Eng. Med., 217: 429-47. DOI: 10.1243/09544110360729072

Unger, E.C., T. Porter, W. Culp, R. Labell and T. Matsunaga *et al*., 2004. Therapeutic applications of lipid-coated microbubbles. Adv. Drug Deliv. Rev., 56: 1291-314. DOI: 10.1016/j.addr.2003.12.006

Zhang, Z., G. Chen, X. Gong, X. Xi and J. Wu *et al*., 2009. A dual-frequency excitation technique for enhancing the sub-harmonic emission from encapsulated microbubbles. Phys. Med. Biol., 54: 4257-72. DOI: 10.1088/0031-9155/54/13/019

Zhu, Y., C. Li, J. Shen, X. Yang and Y. Jing, 2010. Ultrasound-triggered smart drug release from multifunctional core-shell capsules one-step fabricated by coaxial electrospray method. Langmuir., 27: 1175-80. DOI: 10.1021/la1042734